CLASSIFICATION AND FILTERING OF LASER DATA

Carla Nardinocchi [a], Gianfranco Forlani [b], Primo Zingaretti [c]

[a] Dept. ITS, University Roma La Sapienza, Rome, Italy
[b] Dept. of Civil Eng., Parma University, Italy
[c] Dept. of Computer Science, Ancona University, Italy

Commission III, WG 3

KEY WORDS: LIDAR, Classification, Algorithms, DEM/DTM, Automation

ABSTRACT

A strategy for the classification of raw LIDAR data as terrain, buildings and vegetation is presented. Its main features are a preliminary classification of grid data based on a geometric and topological description and a final filtering of raw data, guided by the previous classification. After raw data have been interpolated to a grid and segmented in connected regions bordered by a step edge, the topology of these regions is built up. Noise, vegetation and data gaps are classified first, mainly based on size and region fragmentation. Then, regions enclosing terrain and building points are labelled analysing their relationships with adjacent regions. Since regions may enclose more than one instance of different classes, a first check is made on grid data looking for consistency of gradient orientation with class characteristics. Finally, a local analysis is performed on each grid cell to label raw data point, based on the information on the surroundings inferred by the classification.
Results obtained with Toposys and Optech systems on datasets with different ground point density gathered over the town of Pavia are shown to illustrate the effectiveness of the procedure.

1. INTRODUCTION

Demand for high accuracy, high resolution DTMs in a wide range of applications in civil engineering, environment protection and planning is growing in Italy, pushed by raising standards (e.g. more reliable cost estimation of earthworks in road building) and the development of improved prediction techniques for hydro-geological risk assessment and delimitation of areas subject to flooding. Currently available elevations databases and DTMs come mainly from digitisation of technical maps at scales ranging from 1:5.000 to 1:25.000, whose accuracy standards cannot match those of the new applications. To fulfil this demand, LIDAR is probably still the most effective data acquisition technology, though integrated IMU/GPS systems and digital aerial cameras may narrow the gap in the level of automation of the workflow. Because of its characteristics (first and last pulse, penetration rate in forested areas, etc), LIDAR is anyway better suited and more versatile than photogrammetry for DTM production, breaklines extraction apart. However the accuracy potential of the system is not yet fully translated into DTM accuracy: strip adjustment and georeferencing (including computation of orthometric heights) still deserve attention in pre-processing. Several techniques have been suggested to address these problems and remove systematic errors (Kilian et al. 1996, Vosselman and Maas 2001, Burman 2002).
To remove non terrain data points, interactive editing is still necessary because data classification techniques often fail, increasing production times: there is great interest in developing effective and reliable tools and algorithms on this topic.
Kraus & Pfeifer (1998) filter out trees in forested areas by fitting an interpolating surface to the data and using an iterative least squares scheme to bring down the contribution of points above the surface, so that it gets closer and closer to the lowest data points. Rottersteiner & Briese (2002) stretched this technique to filter out also buildings. Separation of terrain points is achieved by iterative threshold-dependent densification of a TIN (Axelsson, 2000) or by slope based filtering using mathematical morphology (Vosselman and Maas, 2001), the slope threshold being the maximum allowed height difference between two points expressed as a function of the distance between these points. Based on curvature and height difference analysis, Filin (2002) develops a method for clustering data points in surface categories (such as low and high vegetation, smooth and planar surface). With the same goal, Roggero (2001) clusters points based on connectivity and a principal component analisys using geometric descriptors such as static moments, curvature and data anysotropy. Brovelli et al. (2002) filter out non-terrain points by analysing the residuals from a spline interpolation
In the following sections we present our strategy for classification and filtering of LIDAR data for DTM generation. Grown out of a previous (and still ongoing) work on building reconstruction from laser data, our strategy has two distinctive features. In a first stage, raw data are interpolated to a grid, segmented based on height differences and classified in three main classes. In a second and final stage we go back to raw data, filtering points within each grid cell based on the previous classification.
We believe that the aggregation of data in sets enables reasoning about their relationships at an appropriate scale and provides the contextual information essential to increases the probability of correct classification of single data point in the final stage. In this respect we share the motivations of Filin in his proposal and believe that effective filtering cannot be separated by some sort of object recognition: identifying terrain patches or trees is not different from extracting buildings. Though not pretending to be any close to that goal, we are

developing a hierarchical rule-based scheme to classify each region as terrain, vegetation, building and other minor classes. In this respect, it is essential to the viability of the method the segmentation of the data set in connected regions and the reconstruction of the geometric and topological relationships between these regions.
Work is still in progress, so not all rules are yet complete and all cases of ambiguity solved, but results on several datasets are encouraging.
In section 3 we describe in more detail our strategy. Raw data are first interpolated to a grid (3.1); then a region growing algorithm is applied (3.2), which find connected regions bounded by a discontinuity. The topological and geometric description of the regions (3.3) make it easier to apply a set of rules for classification (3.4). Information on gradient orientation (3.5) is used to separate instances of different classes possibly included in the same region. Raw data consistency with cell class (3.6) is finally evaluated. The results shown in section 3 refer to two sites of the of the Pavia dataset, whose characteristics will be presented in the next section.

2. THE PAVIA DATA SET

Under a national research project aiming at the assessment of LIDAR technology for DTM production, height data were acquired in November 1999 over the city of Pavia with an airborne Toposys laser scanning system and, about two weeks later, with a helicopter-based Optech1210 system. Stereo aerial images were also gathered during the Toposys flight. The area covered is about 30 km^2 large and includes the old city centre, with narrows streets and very complex roof shapes, suburban areas with both high rise buildings and detached houses with trees, the Ticino river in the southern part of the town and the countryside with farms, open fields and forests.
The Toposys instrument flew several strips in East-West direction at about 800 m above ground and two cross strips at 400 m with a scan angle of 14°. The point density is about 6 pts/m^2 and 12 pts/m^2 respectively. Only last pulse data were recorded.
The Optech ALTM 1210 instrument flew three missions: the first one covered the urban area at about 600 m above ground with a scan angle of 30° (point density: 1pts/m^2); the second one over a suburban area at about 650 m with a scan angle of 40° (point density: 0.4 pts/m^2) and the last mission along a railway line at about 500 m with a scan angle of 20° (point density: 2.8 pts/m^2). All missions acquired first and last pulse.
Currently we do not perform any strip adjustment: therefore the data we processed are either grid data, registered and interpolated by the data provider (the whole Toposys dataset) or raw data within a single strip (Optech). In the following, the results refer to two areas extracted from the grid data of the Toposys flight at 800 m and from the Optech flight at 600 m.

3. FILTERING TERRAIN POINTS FROM LASER DATA

We want to classify objects in three main classes: terrain, buildings, vegetation, plus other minor classes.
In a primary segmentation we use height differences only, looking for regions separated by a step edge from the adjacent ones. With a proper choice of the threshold, this achieves a good separation of objects.
The classification is performed by a set of rules, based on the geometric characteristic of each region and their topological relationships, where adjacency relationships and height differences along the region borders play a key role. To favour this process we therefore interpolate the raw data to a grid.
The primary segmentation cannot separate all instances of the above mentioned categories; a region may enclose objects of different classes (for instance, a building can be enclosed in the same region with vegetation); on the other hand, the terrain will be likely split in many regions, each of which must be recognized as such and merged. This is achieved with a geometric and topological description of the segmented regions and a further segmentation based on the orientation of the height gradient .
Finally, we go back to the original raw data: we believe that discriminating between points within a mesh element is made easier once its surroundings have been classified with a certain degree of confidence. Therefore, if there is evidence, we filter out non terrain points from regions classified as terrain and, viceversa, label as terrain some points included in regions classified as vegetation. Though currently we have good results working with grid data, we want the region growing algorithm to be independent of the interpolation and to test it directly with raw data.

3.1 Raw Data interpolation

We started working on raw data only lately, so raw data interpolation is still work in progress. We have to answer 3 questions: a) which grid spacing to use; b) what kind of interpolation to use when several raw data points fall into a grid element or when none does; c) how to handle data gaps.
a) The mesh size depends on raw data point density and on the size of the smallest feature to be filtered out. Of course the ground pattern of laser spots plays a major role: the rather anisotropic distribution of the Toposys instrument requires a compromise between the number of points/cells and the percentage of empty cells. Ideally, with a uniform distribution on points on the ground, we would use 1 point/cell: in such case there is no distinction between raw and grid data. With anisotropic data we will have empty cells and cells with many points; points in the latter will be to classified in the last stage. With the Pavia dataset we used 1x1 m mesh size both with Toposys and Optech data.
b) If the cell is empty we currently interpolate with the median of the 8- or 24-connected neighbours. With more than one point the interpolation algorithm may be set to privilege the lower points in DTM generation or the higher points in building extraction, if there is evidence of a step edge; otherwise the median is used. If the cell has just one point we use nearest neighbour interpolation.
c) The philosophy is not to fill gaps larger than 3x3 cells. Data gaps are considered much as regions with no laser response and classified as water.

3.2 Grid Data Segmentation

Grid data segmentation is performed by aggregation of pixels in connected sets, by a region growing algorithm. From a seed pixel, every of the 8-connected neighbours with a height difference with the central pixel less than a threshold is enclosed in the region and becomes in turn seed point of the same region. The process goes on, until no points are added. Therefore, the region border will feature a discontinuity larger

than the threshold. This does not rule out large discontinuities within the region: the algorithm searches all directions to find where the slope is smaller than the threshold. Therefore, if there is a path smooth enough, it can for instance go round very steep terrain breaklines, coming to the top from behind. Ideally, this procedure may include all terrain points in a single region, if there are no closed breaklines steeper than the threshold. With the grid size of one meter, the threshold was set, after some trials (Nardinocchi & Forlani, 2001), to 0.5 m. Originally tuned for building detection, this value has proven to be very effective in sorting out buildings and trees from the terrain. A higher threshold would have made it possible for the algorithm to climb over buildings from nearby trees and also include in the same region several adjacent buildings, making their reconstruction later more complex. The low value cause the trees to be fragmented in many adjacent regions, each made of a few pixels only. The drawback is that the terrain may be split in several regions, because it can be fragmented for instance by dense tree rows, buildings or rivers: labelling regions as terrain is therefore the real task after this preliminary segmentation.

3.3 Geometric and Topological description of the regions

A geometric and topological description of the regions is a key aspect of our approach. For each region, basic statistical parameters are computed. The topological information can be summarised in two graphs: the graph of external adjacencies (*EAG)* and the graph of heights *(HG*) and in a quantitative measure, the useful external border (*UEB*) of a region, defined as the number of pixels that surround (do not belong to) the region and exist (do not belong to the image external border).
Let A_n be a set of simply or multiply connected regions in a plane. An adjacency relationship (*AR)* between two regions A_1 and A_2 exists if and only if the *UEB* of A_1 and A_2 have a non empty intersection. *AR* is reflexive and symmetric. If the *UEB* is visited clockwise (so that the region is always to the right of the border), we can say that A_2 has an external adjacency relationship (*EAR)* with A_1 when A_2 is always on the left of the external border of A_1. According to this definition, *EAR* is transitive but neither reflexive nor symmetric. The unique difference between our *EAG* and a usual adjacency graph (in which nodes represent the regions and arcs, bi-directional or, equivalently, not oriented, the adjacency relationships) is that the arcs must be oriented: if A_1 *EAR* A_2 and A_2 *EAR* A_1 are both true (this is not mandatory) the two nodes must be connected by two opposite arcs, not by one bi-directional arc.

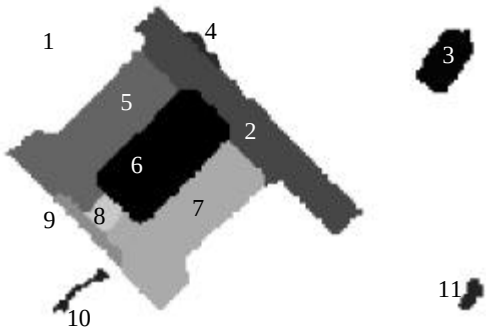

Fig. 1. A typical result of the segmentation process

HG has the same number of nodes, representing the regions, of *EAG*. The arcs of *HG* are oriented from the node corresponding to the region with the higher mean elevation along the common border towards the lower one. In addition, an arc between two nodes exists only if *AR* is true and the difference between the mean heights is an attribute of the arc.
Fig. 1 shows a typical result of the segmentation. Region 1 is the terrain, region 6 a courtyard, region 4, 10, 11 small regions (noise) and the remaining are buildings. The *EAG* and the *HG* of these 11 regions are shown in Fig. 2 and Fig. 3, respectively. This example shows clearly how the above defined topological information can be used in data classification. According to

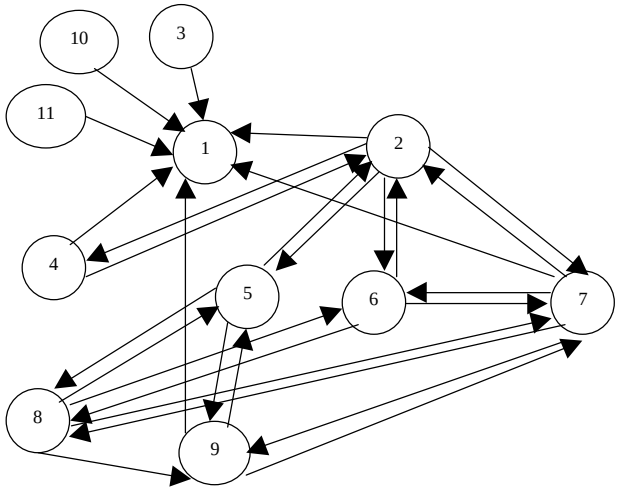

Fig. 2. The EAG of the regions shown in Fig. 1.

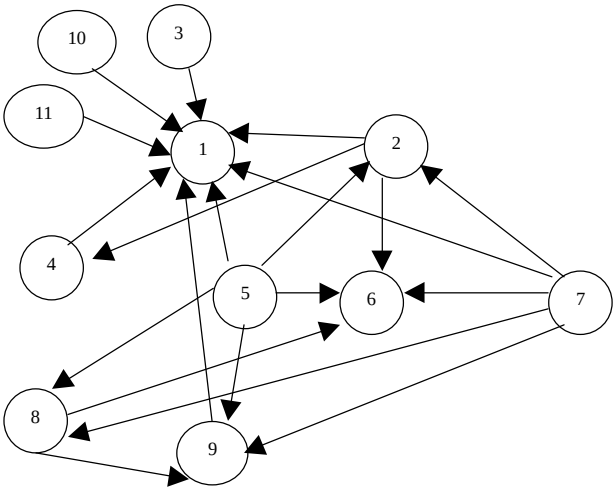

Fig. 3. The HG of the regions shown in Fig. 1

rules in (3.4) , the algorithm is not misguided by the fact that regions 2, 4, 8 and 9 are all surrounded by both lower and higher regions and it correctly classifies them. Labelling of regions 1 and 6, from one hand, and of regions 3, 5, 7, 10 and 11, on the other hand, is straightforward because their nodes in *HG* have, respectively, ingoing and outgoing arcs only.

3.4 Grid Data Classification

The hierarchical application of a set of rules based on the geometric and topologic properties allows to assign regions to

several classes: bare terrain, buildings, vegetation, courtyards, water (or data gaps), narrow regions and noise.

3.4.1 Vegetation and noise. Because of the characteristic of our region growing algorithm the identification of vegetation and noise is straightforward. We define small regions those enclosing less than 3 pixels: if they are adjacent to other small regions, they are grouped together and classified as vegetation; if they are isolated, they are considered as noise.

If first and last pulse are both available (as grid data), they are used to improve the classification. Connected sets of pixels with differences between heights of the first and last pulse larger than 20 cm (i.e. the Z noise level of the sensor) are generated and classified as well as vegetation.

Narrow regions are often found within trees as well as on dykes, fences, balconies, shelters, canopies, etc. They are not yet currently classified as artificial or natural structures.

3.4.2 Terrain. The most significant region with respect to geometric and shape descriptors (max number of pixels, max bounding rectangle) as well as topological relationships (max number of *AR*) is classified as terrain. Other regions exceeding a size of 200000 m^2 are also classified as terrain, provided that all their *EAR* do not have a mean height difference larger than 5 meters (i.e. they are not large industrial buildings). The rationale for this is that, unless small patches are considered (e.g. around a large building block in urban areas), this is always the case.

The terrain may get fragmented in several regions because of "fences", i.e. data gaps, row of trees or large hedges already classified, or by terrain breaklines larger than the threshold. Looking through the *EAG* we are able to verify whether the height difference between the terrain border and the unclassified region border is less than a threshold of 1.5 m, which is less than anything may be called a building and still enough to overcome rows of trees and bushes. Other regions, usually very small, with ingoing arcs only in the *HG* graph are also classified as either terrain or as courtyards, if their adjacent regions are only buildings.

3.4.3 Buildings. Buildings are defined as regions with outgoing arcs only in the *HG*; besides, buildings are identified in two later stages by examining the region's relationships (both in the *EAG* and *HG*) with the previously detected terrain and building regions. Whether or not a region classified as building is really so will be decided later by the building reconstruction module, where, based on clustering of pixels within the same partition of the gradient orientation, roof slopes will be detected. This automatically discards those regions erroneously classified as buildings on high trees with dense canopy.

3.4.4 Others. Some small regions may remain unclassified. They are mainly terrain patches enclosed by vegetation or terrain breaklines. Therefore we label them provisionally as terrain, deferring the final classification to the filtering terrain module.

3.4.5 Two examples. In the following we show the results of the classification for either Toposys and Optech data in two sites drawn from the processing of the whole Pavia dataset. We used grid data provided by Toposys (so we don't know exactly what sort of smoothing has been performed) and raw data, interpolated by the median filtering, for the Optech data; grid spacing is 1 m in both cases.

The first site is the block of the university of Pavia (see Fig. 4): there are many courtyards with trees, narrow streets and cars in the parking area; the second one is a suburban area (see Fig. 7): low rise buildings with surrounding trees and fields bordered by trees. The result of the classification is represented in a colour coded image: buildings detected in separate stages are in white (first stage, regions with only outgoing arcs in *HG*) blue and brown (second and third detection stage); the main region labelled as terrain is represented in yellow, other regions also classified as such are in red; courtyards are in light green. Vegetation is represented in dark green and elongated regions in orange (they look relatively large clusters of pixels, but are in fact made of many small adjacent regions).

Fig. 4 Arial image of the University of Pavia

In the urban scene (Fig. 5 and 6), since Toposys has a higher point density than Optech, interpolation to the grid yields more smoothing: cars in the parking area are not visible, because they have been included in the terrain regions. The same applies, to some extent, to small trees within the courtyards. On the contrary in Optech data the same cars are identified and labelled as "noise". Unclassified regions (the courtyard in top right of Fig. 5) are in grey. The main buildings are correctly extracted in two or three stages (first the towers are selected, then the main block roofs); the tops of three trees are also classified as such, but will be discarded later in the building extraction module.

Fig. 5. Toposys data: classification of the University area

Some buildings (e.g. the small one in the image top) were detected in the first stage with Toposys and in the third stage with Optech data because the interpolation gave rise to a different adjacency graph and triggered a different rule.

Two out of the three narrow (about 5x5x40 m) medieval towers in the centre-right of Fig. 4 (you may spot them from the shadow projected on the main parking area) have been captured in the Optech data as buildings; the third is labelled

as small elongated region. In Toposys data, interpolation probably led to fragmentation of high differences: all towers are marked also as small elongated regions. Optech data also captured more clearly noise and vegetation in courtyards.

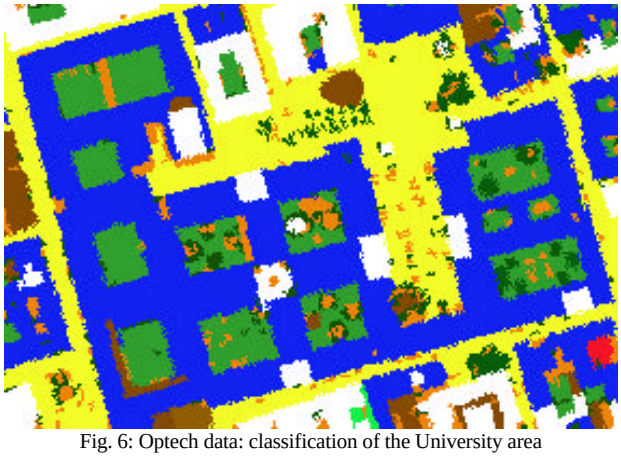

Fig. 6: Optech data: classification of the University area

In the suburban scene (Fig. 8 and 9), grid Toposys data already filtered out much of the vegetation in the lower right corner of the image, because of the higher density and penetration rate in the foliage, so the main terrain region in Toposys is larger. Not so with Optech data, despite first and large pulse were available, probably because of the lower laser spot density.

Fig 7. Aerial image of a suburban area

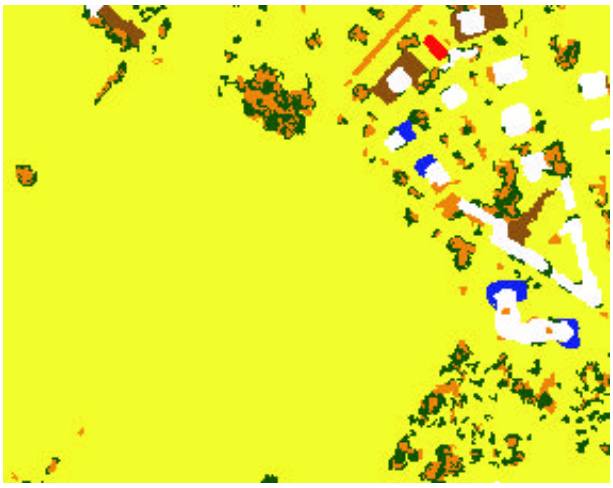

Fig. 8. Toposys data: classification of a suburban area

As far as building identification is concerned, also here different rules were applied but there is considerable agreement between the two outcomes of the classification. Notice that in the Toposys data the car boxes in the top center of the image are missing.

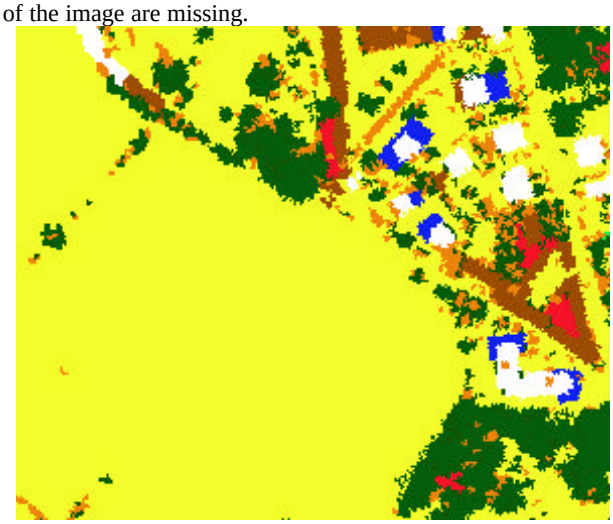

Fig. 9. Optech data: classification of the suburban area

The growing algorithm may have enclosed in regions classified as terrain also non terrain points such as low vegetation or cars and even buildings. When the size of these objects with respect to the grid mesh is large enough, they will show as blobs in the terrain. A further classification and filtering is therefore applied (3.5). To show how it works, we concentrate first of all on the University building and specifically on the courtyards. Figure 10 shows the labels attributed to the courtyards and Table 11 and 12 summarize the main parameters for the region classified as terrain within each courtyard, before filtering.

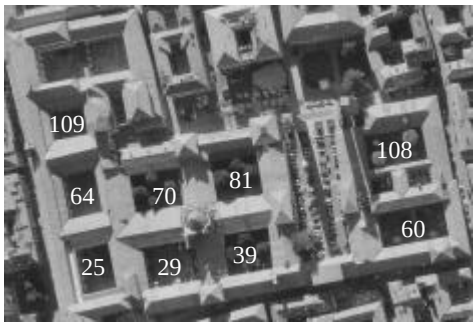

Fig. 12. The courtyards labelled in Table 11

id	# pixels	mean (m)	min (m)	max (m)	σ(m)
25	615	78.19	77.94	80.03	0.28
29	807	78.50	78.22	80.42	0.34
39	503	78.71	78.57	79.19	0.10
60	858	77.96	77.70	79.55	0.16
64	645	77.99	77.86	78.75	0.09
70	459	78.73	78.51	80.36	0.28
81	281	78.63	78.45	79.92	0.19
108	687	78.53	78.35	79.88	0.17
109	428	77.83	77.68	79.83	0.19

Table 11. Toposys data for the 9 courtyards, before filtering

id	# pixels	mean (m)	min (m)	max (m)	σ(m)
25	518	78.22	77.86	80.37	0.34
29	624	78.42	78.12	79.79	0.24
39	406	78.76	78.58	79.57	0.09
60	572	77.91	77.49	78.81	0.12
64	490	78.00	77.76	78.76	0.10
70	349	78.64	78.38	79.04	0.17
81	197	78.66	78.49	78.80	0.05
108	523	78.47	78.21	79.30	0.14
109	368	77.77	77.58	77.97	0.18

Table 12. Optech data for the 9 courtyards, before filtering

Differences in size depends on the larger number of small regions found in Optech, which are basically raw data and moreover on the smoothing applied to Toposys data by the data producer: we have chechek that this results in the systematic underestimation of the building's size. Therefore all courtyard in Toposys data have about 100 pixels more than in Optech. Apart from this, the overall the range and dispersion in elevation of the two sets is similar.
Figure 13 shows a zoom on court 25 for both sets, for the terrain region only: the hole in Optech is a set classified as narrow region.

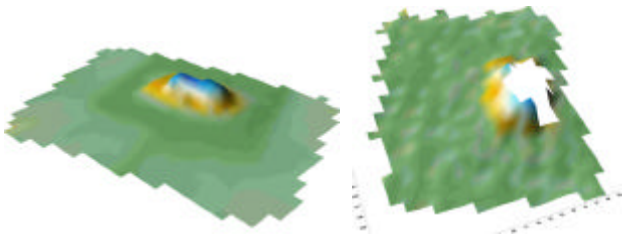

Figure 13. Court 25 before filtering; left :Toposys, right: Optech

3.5 Check on Terrain Data Classification

The idea is to look whether the region is really smooth enough to represent the terrain. To this aim we threshold with a rather low value (0.25) the height gradient and cluster the pixels with similar value of the gradient orientation (we use partitions 45° wide) in new sub-regions. In flat and hilly areas (those where using laser scanning for high accuracy DTM makes sense) the terrain can indeed be assumed to be smooth enough: sudden slope changes may be expected only along break-lines. Therefore, we classify the sub-regions as noise (cars or low vegetation) if smaller than 3 pixels and as breaklines if they are elongated. Buildings may get included in the terrain e.g. when there are car ramps leading to the roof; there is also a (very small) probability that the algorithm climbs on the roof from nearby dense high vegetation. In both cases, there is to be evidence of plane surfaces compatible with a building. Currently, no rule is implemented to solve for this ambiguity.

Figure 14 shows the gradient orientation for the University building, where the same colour correspond to the same class of the partition of the orientation space [0-π]. Orientation has been computed just over the region classified as terrain; black pixels are locally flat, i.e. below the threshold.

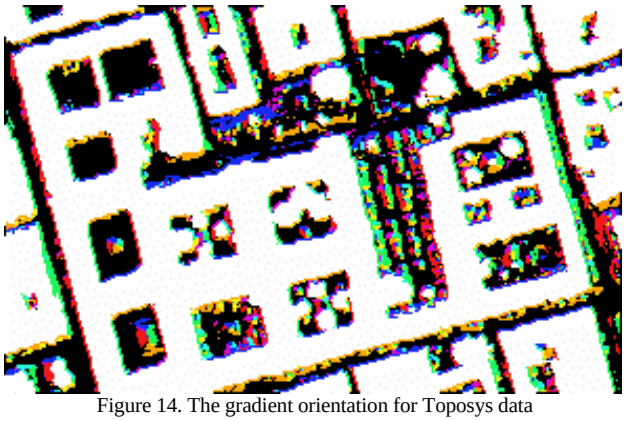

Figure 14. The gradient orientation for Toposys data

As it is apparent, along the building contour there is always a border of pixels with the same orientation: this is because using Sobel operator the height gradient includes also a roof pixel. Within the courtyards the gradient orientation highlights features previously unnoticed by the region growing: some are due to statues or fountains, others to cars parked inside. Also in the main region classified as terrain rows of cars can be noticed.

id	# pixels	mean (m)	min (m)	max (m)	σ(m)
25	377	78.11	77.98	78.28	0.06
29	294	78.29	78.22	78.44	0.13
39	199	78.68	78.57	78.76	0.06
60	456	77.92	77.70	78.14	0.11
64	485	77.96	77.86	78.10	0.06
70	170	78.61	78.52	78.74	0.05
81	156	78.59	78.47	78.68	0.06
108	186	78.47	78.37	78.63	0.05
109	325	77.79	77.68	77.86	0.03

Table 15. Toposys data for the 9 courtyards, after filtering

classe	punti	zmed	zmin	zmax	zsqm
25	329	78.15	77.88	78.65	0.09
29	375	78.36	78.14	79.17	0.19
39	164	78.79	78.62	79.48	0.14
60	198	77.88	77.49	78.40	0.14
64	367	77.98	77.76	78.76	0.06
70	139	78.62	78.41	78.91	0.11
81	78	78.66	78.54	78.77	0.03
108	200	78.45	78.23	79.03	0.07
109	265	77.75	77.58	77.91	0.08

Table 16. Optech data for the 9 courtyards, after filtering

Table 15 and 16 summarize the results of this further classification in the courtyards: the final terrain region has been sharply reduced in both datasets. As can be seen, even accounting for the above mentioned difference in size of the courtyard, more points have been discarded in Optech than in Toposys. Despite this Optech remain more noisy (we should not forget that Toposys has a higher density and was gridded with some smoothing). This point out to the need to try to get back some of these points in the final filtering stage. Figure 17 show the enlarged view of court 25 after filtering.

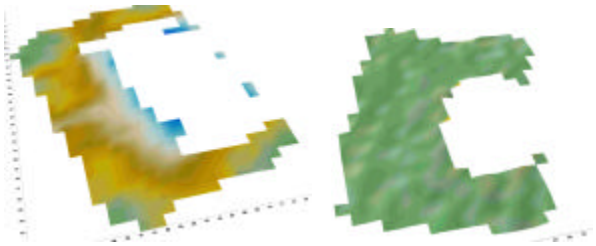

Figure 17. Court 25 after filtering; left :Toposys, right: Optech

It is apparent that the grid interpolation with Toposys results in a larger

Coming back to the two larger areas, Fig. 18-21 show the results of this further filtering: pixels definitely assigned to terrain are in yellow, buildings are in blue, vegetation in green and orange pixels are elongated regions; pixels discarded using gradient orientation are shown in pink (small regions) and black (breaklines). Small elongated regions (orange) are still unclassified. This is deferred to the final filtering, going back to raw data.
In the urban scene, all buildings have been found; vegetation has always been well detected using a single impulse response; noise, such as cars, has also been successfully detected in this step of terrain filtering. As noticed earlier, trees in blue will be discarded later, when consistency with a plane will be tested.

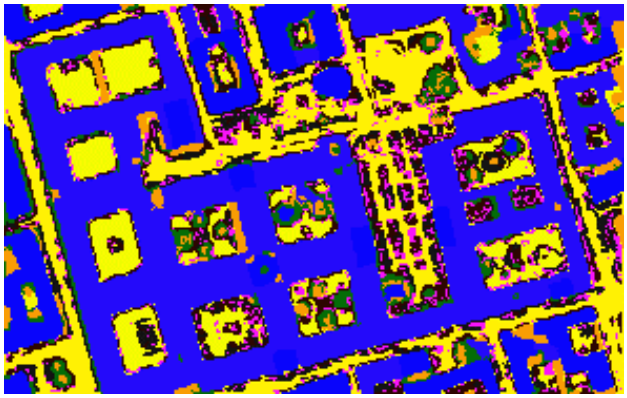

Fig. 18. Toposys data: result of terrain extraction

In the urban scene, all buildings have been found; vegetation has always been well detected using a single impulse response; noise, such as cars, has also been successfully detected in this step of terrain filtering. As noticed earlier, trees labelled in blue will be discarded later, when consistency with a plane will be tested.

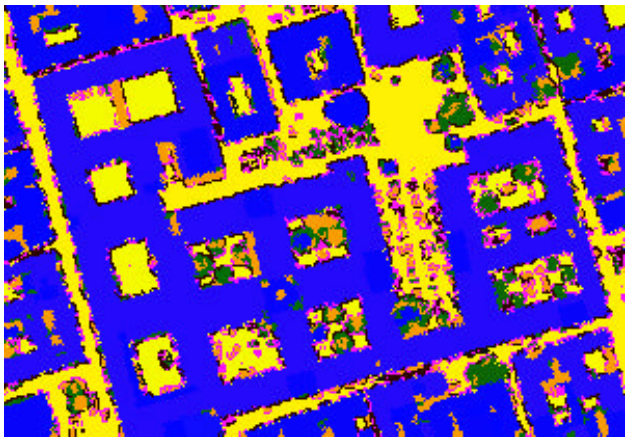

Fig. 19. Optech data: result of terrain extraction

Also in the suburban area all main buildings have been found, despite more disturbances by nearby trees. Boxes in the top center of the image where identified in Optech and not in Toposys data. Filtering with gradient orientation highlighted some of the vegetation undetected by the height difference segmentation in Toposys data. Overall, the results look quite similar in both datasets.

3.6 Raw Data Classification

The main task of this last filtering stage is to extract terrain points in regions classified as vegetation, either rows of trees or forested areas: this is still work in progress. To this aim we plan to check the region border from adjacent regions classified as terrain, looking for consistency of the points in the border cells with the terrain just outside. This also applies, but in a simpler manner, to points labeled as noisy data within areas classified as terrain: in case there is redundancy in the cell (i.e. there is more than one point) we look whether some point may in fact belong to the terrain. Finally, also regions classified as terrain will be checked, again in case of redundancy, if their Z values lie within a given range with respect to the interpolated height of the pixel.

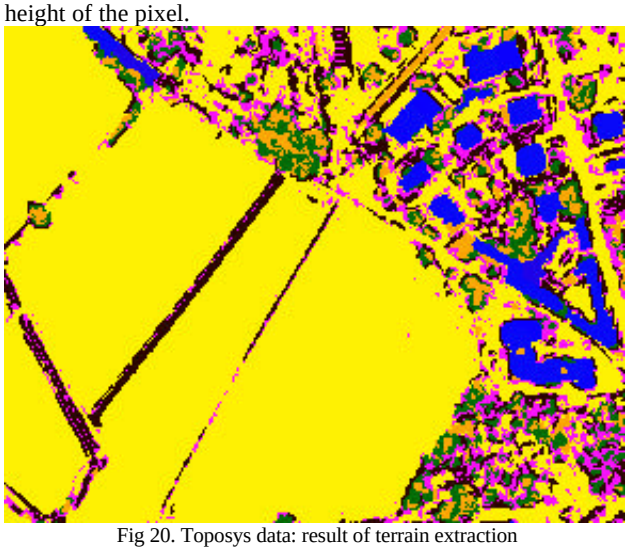

Fig 20. Toposys data: result of terrain extraction

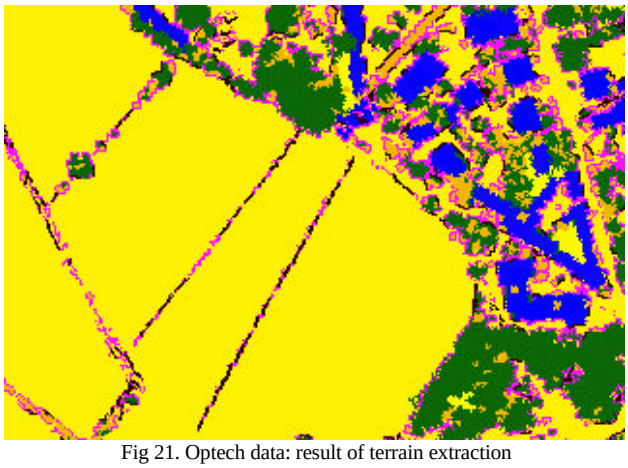

Fig 21. Optech data: result of terrain extraction

4. CONCLUSIONS AND PERSPECTIVES

Originally developed for building extraction and reconstruction (and still integrated in the same software), a strategy for automatic data classification of LIDAR data has been presented. As already remarked, work is still in progress: grid interpolation and the final filtering within each cell have not been fully addressed yet. The core of the procedure, i.e. the classification of grid data based on their geometric and topological relationships and the filtering with gradient orientation look sound enough. Although contextual information may be recovered correctly, some ambiguities will obviously never be solved, because the variety of situations in real world cannot be squeezed in a few rules; we are also aware of the risk of being misled by the particular dataset the strategy is tested on. The reliable identification of the main terrain regions is perhaps the most important aspect the method relies on implicitely, especially for the success of the final filtering. The order the rules are being applied is also important, especially when not all neighbouring regions have been already classified: we want to gain more experience on that. Overall, results are more than encouraging.

Besides the large Pavia dataset, processed with two different laser systems, the method has currently been applied to other datasets, including those provided for the ISPRS WGIII/3. Here examples of rough terrain were also processed, demonstrating that the method can deal with dataset containing many breaklines.

From the very preliminary comparison we made, using both first and last pulse or just last pulse doesn't seem to change much the results, therefore the classification of the vegetation is good enough: the only difference is that the amount of small or elongated regions is clearly larger when using both first and last pulse, because the threshold we used (0.2 m) is less than that of region growing, so fragmentation gets higher.

We want to improve the effectiveness of the preliminary interpolation over the grid trying different kind of filters and to study the behaviour of the algorithm under different laser spot densities and grid size.

Acknowledgements

This work has been partly financed under the national research project COFIN n. 9808229941_002.

References from Other Literature:

Axelsson, P., 2000. DEM generation form Laser Scanner Data Using Adaptive TIN Models. International Archives of Photogrammetry and Remote Sensing, Vol. 33 B4/1 pp. 110-117.

Brovelli, M.A., Cannata, M. Longoni, U.M., 2002 Managing and processing LIDAR data within GRASS. Proc: Open source GIS - GRASS users conference. Trento, Italy, 11-13 Sept. 2002 Burman, H., 2002. Laser Strip Adjustment for Data Calibration and Verification. International Archives of Photogrammetry and Remote Sensing, Vol. 34/3 A, Graz, Austria, 2002.

Filin, S. 2002, Surface Clustering from Airborne Laser Scanning Data. In: International Archives of Photogrammetry and Remote Sensing, Vol. 34/3 A, Graz, Austria, 2002.

Kraus, K., Pfeifer, N., 1998. Determination of Terrain Models in Wooded Areas with Airborne Laser Scanner Data, ISPRS Journal of Photogrammetry & Remote Sensing, vol. 53, pp. 193-203.

Kilian, J., Haala, N., Englich, M., 1996. Capture and evaluation of airborne laser scanner data. In: International Archives of Photogrammetry and Remote Sensing, Vol. 31/B3, Vienna, pp. 383-388.

Nardinocchi C., Forlani G., 2001. Detection and Segmentation of Building Roofs from Lidar Data. ISPRS Workshop on 3D Digital Imaging and Modelling Applications of: Heritage, Industries, Medicine & Commercial Land, Padova, 3-4 April 2001.

Roggero, M., 2002. Object segmentation with region growing and principal component analysis. International Archives of Photogrammetry and Remote Sensing, Vol. 34, Part 3A, Graz, Austria.

Rottensteiner, F., Briese, Ch., 2002. A new method for building extraction in urban areas from high-resolution LIDAR data. International Archives of Photogrammetry and Remote Sensing, Vol. 34, Part 3A, Graz, Austria.

Vosselman, G., Maas, H.-G., 2001. Adjustment and filtering of raw laser altimetry data. OEEPE Workshop on Airborne Laserscanning and Interferometric SAR for Detailed Digital Elevation Models, Stockholm, 1-3 March 2001, Official Publication OEEPE no. 40, 2001, pp. 62-72.